Doménech-Carbó, A.; Holmwood, S.; Di Turo, F.; Montoya, N.; Valle-Algarra, FM.; Edwards, HG.; Domenech Carbo, MT. (2019). Composition and Color of Maya Blue: Reexamination of Literature Data Based On the Dehydroindigo Model. The Journal of Physical Chemistry C. 123(1):770-782. https://doi.org/10.1021/acs.jpcc.8b08448

On the Composition and Color of Maya Blue: A Reexamination of Literature Data Based on the Dehydroindigo Model

Antonio Doménech-Carbó[a]*, Sigrid Holmwood[a], Francesca Di Turo[b], Noemí Montoya[a], Francisco Manuel Valle-Algarra[a], Howell G.M. Edwards[c], María Teresa Doménech-Carbó[d]

[a] Departament de Química Analítica. Universitat de València. Dr. Moliner, 50, 46100 Burjassot (València) Spain.
[b] Department of Earth Sciences, Sapienza University of Rome, P.le Aldo Moro 5, Rome, Italy.
[c] Department of Chemical and Forensic Sciences, University of Bradford, Bradford BD7 1DP, U.K
[d] Institut de Restauració del Patrimoni, Universitat Politècnica de València, Camí de Vera 14, 46022, València, Spain.

* Corresponding author. E-mail: antonio.domenech@uv.es

Abstract

An analysis of literature data studying the composition and color of Maya blue (MB) type materials prepared from indigo, dehydroindigo and different aluminosilicates, accompanied by new spectral data, is presented. After thermal treatment at above 100 ºC, indigo-based specimens displayed Raman and UV-Vis spectroscopic features common to those of equivalent dehydroindigo-based replicants, thus supporting the so-called dehydroindigo model (*J. Phys. Chem. B* **2006**, *110*, 6027-6039) in which the dehydroindigo/indigo ratio, increasing with temperature, is crucial to determine the color of MB and its variability. The current analysis supports the view of MB as a polyfunctional hybrid material just characterized by the presence of different organic components each one distributed in topological isomers differently attached to the clay support. Based on the comparison of spectral data for different channeled silicates (among others, palygorskite, sepiolite, and montmorillonite clays, and different zeolites), it is proposed a view on the color characteristics of Maya blue-type specimens as defined by the compromise between trapping ability for indigo molecules and facility to promote the oxidation of indigo to dehydroindigo.

Introduction

Discovered in 1931 for the modern science,[1] the Maya blue (MB), a pigment widely used in pre-Columbian times by the Mayas and other ancient Mesoamerican peoples, has received attention because of its enormous stability, characteristic brightness and peculiar hue.[2] Today is recognized as a hybrid organic-inorganic material,[3] an idea initiated by Shepard in the 1960's,[4] produced by associating indigo (3H-indol-3-one-2-(1,3-dihydro-3-oxo-2H-indol-2-ylidene)-1,2-dihydro), a blue dye extracted from leaves of *añil* or *xiuquitlitl* (*Indigofera suffruticosa*), to palygorskite, a layered clay of ideal composition $Si_8(Mg_2Al_2)O_{20}(OH)_2(H_2O)_4 \cdot 4H_2O$. Unfortunately, there is no disposal of historical sources describing the preparation of the pigment and several possibilities have been considered.[2,5-7]

The composition and structure of the pigment has motivated successive discussions in relation to the stability of the pigment, the nature of the indigo-palygorskite association, the location of the dye molecules on the clay support, and the origin and variability of the color. It was proposed that indigo molecules were adsorbed onto the external surface of palygorskite crystals,[8] entrapped into the palygorskite channels,[9-13] blocking the entrances at the edges of palygorskite channels[14,15] and the grooves of channels in the external clay surface.[16]

Similarly, alternative models have been proposed to describe the interaction between indigo and palygorskite, namely, formation of hydrogen bonds between indigo C=O and N-H units with edge silanol units of the clay,[14] hydrogen bonding of such units (mainly C=O) with structural water,[10-12] direct bonding to Al^{3+} substituted Si^{4+} sites in tetrahedral centers[17-19] and to clay octahedral Mg^{2+} and Al^{3+} cations.[13,16]

Such approaches were more or less explicitly dominated by a common view that can be viewed as an 'unicity paradigm' based on the assumption that there is only one dye, indigo, constituting MB, that there is a unique type of anchorage between the clay and the dye and that there was a unique preparation recipe used by the ancient Mesoramerican peoples. In 2006, we provided an alternative view, supported on electrochemical and spectroscopic data, to the above 'unicity paradigm', based on the proposal that dehydroindigo, an oxidized form of indigo of yellow color, accompanies this dye in the MB and that the dehydroindigo/indigo proportion in the

pigment is decisive to determine its hue.[20] The aerobic oxidation of indigo to dehydroindigo was thermodynamically favored so that the presence of different dehydroindigo/indigo ratios, in turn depending on the temperature during the preparation of the hybrid material, would explain the hue variability of the pigment, ranging from dark blue to turquoise green.[20-22] This approach permitted to describe the MB as a polyfunctional hybrid material where different dyes (indigo, dehydroindigo, indirubin, isatin, …) can be associated to different clay sites.[23-25] Data on archaeological samples permitted to propose an evolutionary view of the MB, which could have been prepared using different local recipes, defining a tentative ramified evolutionary scheme,[21,26-28] and permitted to characterize new archaeological materials of the same type.[29-31]

This dehydroindigo (or, better, the multi-organic component) model, although accepted by several groups,[13,18,19,32-35] has not been considered or only partially accepted in much of recent literature,[15,36-41] retaining the idea that indigo is the unique organic component in the MB, in the following, the 'all-indigo' model. The focus in the dehydroindigo model has been made on the presence of other dyes accompanying indigo in MB; although HPLC/MS experiments on MB extracts permitted to characterize unambiguously the presence of dehydroindigo, isatin, etc. as a minority components in MB-type specimens,[42,43] it is no easy to provide an equivalent evidence for the 'internal' dye species. In the more recent contribution within the 'all-indigo' view, De Faria et al.,[44] based on resonance Raman spectroscopy measurements on MB simulants prepared from palygorskite, sepiolite, montmorillonite and laponite, conclude that: i) there is no dehydroindigo in palygorskite-based MB specimens although it is present in laponite and montmorillonite specimens, and ii) there is no contribution of dehydroindigo to the color of the MB.

The purpose of the current report is to discuss the problem of the composition and color of the MB balancing the aforementioned 'all-indigo' and dehydroindigo models. Literature data and new spectral data for different indigo plus clay specimens heated at different temperatures (IND@CLAY$_t$), including palygorskite (PAL), sepiolite (SEP), montmorillonite (MON), and kaolinite (KAO) are presented. Since, to the best of our knowledge, no other electrochemical data than those provided by our research group have been reported, such data –all confirming the dehydroindigo model-[20-26,42,43] have been omitted. The current study is focused in the aforementioned composition and color problems, with abstraction of other related problems: the

location of organic molecules in the inorganic support and the type(s) of bonding determining their mutual association. The analysis reported here indicates that all available spectral data, including those from Martinetto et al.[38] and De Faria et al.,[44] advocating the 'all-indigo' model, are consistent with the dehydroindigo model.

Experimental details

For preparing MB-type specimens, indigo reagent (Aldrich), palygorskite (collected from Yucatán site of Ticul), sepiolite from Yunclillos (Spain), supplied by Tolsa; montmorillonite and kaolinite (from the Source Clays Repository of the Clay Mineral Society) were used. Different IND@CLAY$_t$ specimens were prepared by crushing and mixing in agate mortar aliquots of ca. 1.0 g of clay plus 1 wt % indigo during 1 h. The powdered mixture was then submitted to heating in furnace at temperatures between 120 and 180 ºC for 24 h. The specimens were successively rinsed with DMSO and acetone to remove the dye remaining 'externally' attached to the clay. Aliquots of ca. 0.2 mg of the IND@CLAY specimens were subjected to extraction with 1 mL of DMSO, and H_2O:MeOH and MeOH:DMSO mixtures in closed vials for 24 h under magnetic stirring.

Chromatograms of the extracts were performed in the gradient mode at a LC-DAD equipment (Agilent 1200 Series HPLC system) using a UV-Vis diode array detector set at 286 nm (Agilent Technologies, Palo Alto, CA, USA). The column was an Agilent Zorbax XDB C18 150x4,6 mm, 5 µm particle size (Agilent) preceded by an Agilent® Zorbax guard cartridge. Signals were processed by Agilent ChemStation software Ver. 10.02 [1757]. The mobile phase (flow rate 1.2 mL min^{-1}) used was a mixture of two solvents (solvent A: water - 0.1 % formic acid and solvent B: acetonitrile). Gradient conditions were initiated by holding the mobile phase composition for 0.1min with 7 % B, after that it was changed linearly to 75 % B during 12 min. The composition was then changed to 98 % B in 3 min and maintained for 4.5 min as a cleaning step in order to improve the results. After cleaning, the eluent composition was returned to the initial 7 % B. The column oven was operated at 35 ºC and the injection volume was 10 µL.

Raman spectra were recorded using a Renishaw *In Via* microRaman spectrometer operating

with a laser excitation wavelength of 785 nm and a spectral resolution of 2 cm^{-1} with 20× objective lens giving the sample a footprint of about 10 microns at the specimen with spectral scans of 10 s and ten accumulations; several regions of each sample were analyzed to achieve reproducibility. Spectra were not treated or subjected to background subtraction.

Diffuse reflectance spectra were obtained with a Perkin-Elmar lambda35 spectrometer, slit width 1 nm, scan speed 480 nm/min, in the case of solutions using 1 cm quartz cells. Deconvolution was carried out using the Magic Plot System software.

Results and discussion

The preparation of MB replicants

Due to the no availability of genuine, archaeological MB samples, the majority of studies are conducted on MB replicants. There are, however, several problems in this regard needing consideration prior to analyze spectral features. First of all, although several 'dry' and 'wet' preparation methods can be used,[5,8,9] in general, crushing solid indigo ca. 1 % wt with palygorskite and heating at temperatures between 100 and 180 ºC was used.[10-44] This procedure results in the maintenance of a significant amount of 'external' indigo, which it is convenient to remove by treating the indigo plus palygorskite material with HNO_3 or an organic solvent such as DMSO. Several authors have prepared materials with higher proportions of indigo (between 5 and 20 % wt) and studied with no 'cleaning'.[15,36,37] By the reasons already discussed,[42,43] this kind of preparations, although interesting as technological materials, cannot be strictly considered as 'genuine' replicants of archaeological MB.

Several studies have been conducted preparing MB-type specimens with sepiolite,[14,24,25,35,36,39,43-45] a phyllosilicate clay of ideal formula $Mg_8Si_{12}O_{30}(OH)_4(OH_2)_4 \cdot nH_2O$ ($n \leq 8$) and other silicates, including montmorillonite,[24,38,43-45] kaolinite,[33,34,46] and silicalite,[37,43,46] among others. Roughly, these studies were mainly devoted to compare the differences in the attachment mode of indigo to the channeled silicates, where there is possibility, as previously noted, of occupation of different sites, and non-channeled silicates, where the organic molecules dispose of less possible association types. It is worth to note that in non-channeled clays, cleaning with HNO_3 or organic solvents produces the removal of the

organic components. For our purposes, it is convenient to note that the presence of dehydroindigo has been reported in hybrid materials prepared by crushing indigo with palygorskite,[20-26,33,42,43] sepiolite,[24,25,43] montmorillonite, [24,25,43,44] kaolinite[43,34] and laponite.[44] In turn, hybrids prepared by crushing dehydroindigo with palygorskite[33,44] and sepiolite, laponite and montmorillonite,[44] have been studied.

Finally, it is important to realize that for obtaining the blue-greenish color characteristic of genuine ('archaeological') MB, the synthetic replicants have to be submitted to heating at temperatures above 100 ºC (usually between 120 and 180 ºC) for different times. This process results in the loss of zeolitic water unanimously considered[10-46] as necessary for the attachment of indigo to the palygorskite framework. The MB replicants will be represented in the following as ORG@CLAY$_t$, ORG denoting the organic component, CLAY the clay and t the temperature of the specimens submitted to heating.

Raman spectroscopy

The Raman spectra of genuine MB samples and/or MB-type synthetic specimens has been studied by different authors.[12,13,41,44-50] Although there are differences depending on the working conditions of the experiment, in particular the excitation wavelength (*vide infra*), there are essentially common spectral features.

Regardless detailed band assignment, there is general agreement in which the spectra of solid indigo and unheated indigo plus palygorskite are similar but that they differ clearly from the spectra of IND@PAL$_{120\text{-}180}$ and IND@SEP$_{120\text{-}180}$ specimens which, in turn, have major similarity with the spectrum of indigo in solution in organic solvents.[12,13,44-50] This feature, also observed in UV-Vis spectrophotometry (*vide infra*) is rationalized on assuming that indigo, although forming bonds with the inorganic host, is mainly forming isolated molecules in the MB so that strong intermolecular hydrogen bonds present in the solid dye are absent. This can be seen in Figure 1, adapted from De Faria et al.[44] where the region between 1200 and 1800 cm^{-1} (this spectral region was selected as being the unique common for all spectra in ref.[44]) of the Raman spectra of a) indigo in DMSO solution (λ_o = 532 nm) after subtraction of the solvent spectrum, b) IND@PAL$_{130}$ (λ_o = 632.8 nm), c) solid dehydroindigo, d) IND@PAL$_{130}$

and e) DHI@SEP (all three using λ_o = 457.9 nm) are compared. Indigo in solution displays bands at 1698, 1627, 1578, 1448, 1362, 1316, and 1248 cm^{-1}, whereas the IND@PAL_{130} specimen yields bands at 1680, 1634, 1595^{sh}, 1576, 1490, 1448, 1378, 1361, 1316, and 1252 cm^{-1}. Apart from the shift of the band at 1698 cm^{-1} to 1680 cm^{-1} and other small shifts, the more relevant features are the appearance of new bands at 1595 (shoulder) 1490 and 1378 cm^{-1} and the significant decrease in the intensity of the band at ca. 1630 cm^{-1}. Notice that the use of different excitation wavelengths results in variations in the relative height of the bands but not (or minimal) in the peak wavelengths.

In the conceptual frame of the 'all-indigo model', all these features are viewed as the result of the interaction of the indigo molecule with the clay framework. In particular, the new bands at 1595 and 1378 cm^{-1} were attributed by Witke et al.[52] to A_g + B_u and B_u δ(N−H) modes associated to the loss of planarity of the indigo molecule. However, the study by Sánchez del Río et al.[45] concluded that: the Raman spectra of MB specimens prepared with palygorskite, sepiolite and montomrillonite and, to a lesser extent, with kaolinite, were similar and that the loss of planarity is not sufficient to explain the features in the Raman spectra of indigo plus clay mixtures.

The 'all-indigo' interpretation of the Raman spectra of MB simulants[41,44,45] becomes weakened when the spectra of indigo replicants are compared to those of dehydroindigo replicants. The spectrum of solid dehydroindigo shows bands at 1732, 1597, 1530, 1448, and 1378 cm^{-1}, thus providing a common band (1448 cm^{-1}) and two bands without equivalent to the above indigo specimens (1732 and 1530 cm^{-1}). However, DHI@PAL_{130} displays just the bands at 1595, 1490, 1461, 1420 and 1378 cm^{-1} appearing in IND@PAL_{130} (and all IND@PAL_t specimens) which are absent in the spectrum of indigo in solution. In particular, the above bands, which in our interpretation characterize dehydroindigo, are enhanced in resonance Raman spectra recorded at λ_o = 457.9 nm relative to the same bands in Raman spectra at λ_o = 632.8 nm, consistently with their correspondence with the visible band at 500 nm, which, in our view, has to be attributed to palygorskite-associated dehydroindigo (see Supplementary information, Figure S.1). This matter will be treated in detail in the next section.

The presence of bands equivalent to those of DHI@PAL_{130} is enhanced when the spectrum of IND@SEP_{130} is considered. As can be seen in Figure 2, this last replicant displays bands at 1680, 1634, 1595, 1574, 1490, 1461, 1378, 1362 and 1252 cm^{-1}, exactly the same that those found at DHI@PAL_{130} with except of their relative intensities and the appearance of the band at 1316 cm^{-1}. As can be seen on comparing the corresponding spectra -(d) and (e) in Figure 1, the spectrum of DHI@PAL_{130} was almost identical to that of IND@SEP_{130} and, in fact, this was clearly similar to those of IND@MON_{130} and IND@LAP_{130} (where De Faria et al. accept the presence of dehydroindigo[44]). Since the bands at 1680, 1634, 1595, 1576, 1490, 1378, 1361, and 1252 cm^{-1}, characterizing the spectrum of the DHI@PAL_{130} specimen, are also present in the Raman spectrum of IND@PAL_{130} replicants (see Figure 1), the more logical conclusion is that, contrary to the interpretation of the same data made by De Faria et al.,[44] dehydroindigo is present, although in different proportions, in IND@PAL_{130} and IND@SEP_{130} specimens.

Table 1 summarizes the bands for solid indigo, indigo in DMSO solution, solid dehydroindigo, IND@PAL_{130}, IND@SEP_{130}, and DHI@PAL_{130} specimens from literature.[44,52,53] One can see that: i) although with significant variations in intensity, common sets of bands at fixed wavenumbers (± 2 cm^{-1}) appear; ii) regardless the intensity of bands, the spectra of solid indigo and solid dehydroindigo do not match with the spectra of the MB-type specimens, in agreement with the idea that the hybrid materials involve the 'molecularization' of the dye (*vide infra*); iii) there is an almost complete matching between the Raman spectra of IND@SEP_{130}, and DHI@PAL_{130} replicants, iv) the Raman sepectra of IND@SEP_{130}, and IND@PAL_{130} also match with the spectrum of DHI@PAL_{130}, in agreement with the presence of a significant proportion of dehydroindigo in MB.[20-31,42,43,50]

Additionally, it is pertinent to mention that indigo, dehydroindigo and other indigoids such as isatin and thioindigo exhibit common IR and Raman bands, as underlined by Tomkinson et al.[51] in their study using both DFT and H-F calculations of the Raman spectra of indigo, thioindigo and isatin. These authors concluded that the absence of the γ(N-H) band at ca. 750 cm^{-1} is the more relevant spectroscopic feature to test the presence of dehydroindigo in MB-type specimens. This means that, if dehydroindigo accompanies indigo in MB, this band should be diminished in the IND@PAL_t specimens relative to those others containing only indigo molecules. This effect can clearly be seen in the Raman spectra depicted in Figure 2,

corresponding to i) solid indigo and ii) IND@SEP$_{150}$, iii) IND@PAL$_{150}$ specimens and can be seen in Raman spectra reported for different IND@CLAY$_t$ hybrids[35,45] and, in particular, for genuine MB specimens from reported by Lamprecht et al.[41] depicted in Figure 3. Although interpreted by these authors in the context of the 'all-indigo' model, the spectra in Figure 3, taken from four blue spots of a Maya clay head figurine of the Ethnological Museum of Berlin (Catalog No. IVCa 21166), display the Raman features coincident with those recorded for DHI@PAL$_t$ replicants, in particular, those at 1680, 1634, 1595, 1490, 1461, 1378 cm^{-1}, absent in the spectrum of indigo in solution. Again consistently with the interpretation of the Raman spectra under the dehydroindigo model view, the N-H characteristic band at 754 cm^{-1} is absent or almost entirely absent in these spectra as expected for samples containing a significant proportion of dehydroindigo.[51]

The composition problem

A first mention of the presence of other organic components accompanying indigo in MB was made by Vandenabeele et al.,[48] reporting the possible presence of leucoindigo accompanying indigo based on Raman spectroscopy data. The presence of dehydroindigo and its relevance for the color of MB was proposed in previous papers where spectroscopic and solid state electrochemistry data supporting this idea were presented.[20-26] In fact, as already reported,[42,43] dehydroindigo, isatin, and other organic components can be isolated and identified from the extracts of IND@PAL$_t$ replicants using different solvents thus denoting that, at least in the 'external' region of the clay, indigo is accompanied by significant amounts of these other dyes. Figure 4 shows LC-UV chromatograms of a) indigo and b) isatin solutions in DMSO, and c) the DMSO extract of IND@PAL$_{180}$ specimen recorded under the conditions described in the Experimental section. The chromatogram of the MB replicant shows the peaks of indigo and isatin accompanied by several other components, including dehydroindigo, as confirmed by the UV-Vis spectra of the eluted aliquots of the chromatograms (d-f) and their characteristic mass spectra obtained in UPLC-MS experiments previously reported (See Supplementary Information, Figure S.2).[42,43] Consistently with the increase of the dehydroindigo/indigo ratio on increasing the temperature of preparation of the MB-type specimens, the ratio of the corresponding chromatographic peaks increases on increasing temperature,[42] see Figure S.3 in Supplementary Information.

The individual components can be also separated and individualized applying conventional extraction procedures to the replicants and our data indicate the presence of other organic components than indigo. This is illustrated in the inset in Figure 4, where the photographic image of the consecutive extracts with (from left to right) 90:10 (v/v) H_2O:MeOH, 50:50 (v/v) MeOH:DMSO, and DMSO of an IND@KAO specimen, are depicted. Consistently, voltammetric data on the DMSO extracts from the above replicants display the characteristic features of indigo, dehydroindigo and isatin coincident with those described in the solid state electrochemistry of different IND@$CLAY_t$ specimens (see Supplementary information, Figure S.4).[20-26]

Following the same line of reasoning, although focused on sepiolite-based replicants, ^{13}C NMR data also supported the presence of dehydroindigo accompanying indigo. Thus, several authors reported the presence of 'translated peaks' at 191 and 138 ppm[14,35,36,39] relative to the carbonyl group resonance (188 ppm) and peripheral C atoms (134 ppm) of indigo, interpreted as being the signals characterizing some clay-complexed indigo forms. However, these signals can correspond to those appearing in the ^{13}C NMR spectrum of dehydroindigo (189.5, 139.1, 136.8).[33] In fact, the ^{13}C NMR spectra of IND@SEP_t replicants (see Figure 5) prepared by different groups[14,35,36,39] show two peaks at 191 and 188 ppm and a weak multiplet centered at 136 ppm, as expected for a system containing indigo plus dehydroindigo (see also Supplementary Information, Table S.1).

Visible spectra

Figure 6 compares the UV-Vis spectra for indigo and dehydroindigo in DMSO solution, solid indigo, and IND@PAL_{130}. In the visible region, indigo solutions in organic solvents display an absorption band whose maximum ranges between 600 (toluene) and 620 nm (DMSO) (Fig. 6a) whereas dehydroindigo solutions ranges between 400 and 455 nm.[33,44,53] In solid state (Fig. 6c), the indigo band is shifted to a maximum of 657 nm, which is accompanied by a shoulder ca. 560 nm. Non-heated indigo plus clay replicants provide spectra which are essentially identical to that of solid indigo, the material retaining the blue tint of the dye.[24,25,33,44,53,54] Upon heating above 100 ºC, the spectra of IND@$CLAY_t$ specimens, which present a more or less greenish hue, are characterized by the shift of the maximum of the main indigo band between ca. 640 nm

(IND@SEP_{130}) and ca. 670 nm (IND@PAL_{130}), and the decrease of the shoulder at ca. 560 nm (see Fig. 6d for IND@PAL_{130}). In this region of wavelengths a new absorption band appears at ca. 500 nm, whose height relative to the ca. 650 band increases on increasing the temperature used for the preparation of the specimen. [24,25,33,44,53] Deconvolution of the spectra permits to their decomposition into different Gaussian components. Although this analysis is merely tentative, the spectra of IND@PAL_t specimens contain components coincident with those for indigo and dehydroindigo in solution (marked by arrows in Fig. 6), in agreement with the idea that individual dye molecules are associated to the palygorskite.

The early studies on the visible spectrum of MB by Leona et al.[47] and Reinen et al.[54] concluded that the interaction of isolated (as opposite to hydrogen bonded molecules in solid indigo) indigo molecules with the palygorskite framework were responsible for the bathochromic shift of the main absorption band and the appearance of the 500 nm band.

The spectral data on dehydroindigo and DHI@PAL replicants[33,44,53] clearly suggests that the 500 nm band can be attributed to clay-associated dehydroindigo (see, in particular, Figure 9 in ref. [33]). Quantum mechanics calculations have been applied to reproduce the spectral features of MB based on different models of the palygorskite-indigo interaction.[13,18,19] These include indigo and dehydroindigo complexes with structural water molecules, direct binding to Mg^{2+} and Al^{3+} cations of the palygorskite framework, respectively formulated as [DYE-$(H_2O)_4Mg]^{2+}$, [DYE-$Mg(H_2O)_4]^{2+}$, and [DYE-$Al(H_2O)_4]^{3+}$ by Tilocca and Fois.[13] In principle, such calculations are consistent with the presence of dehydroindigo in MB[13,18,19] and confirmed the substantial role of this component in the optical properties of MB.[13]

In this scenario, there are two possible views of the 500 nm band determining the color of the MB: in the ‘all-indigo model’, the band is attributed to an unspecified indigo-palygorskite complex;[44] in the dehydroindigo model, this band has to be attributed to the presence of palygorskite-associated dehydroindigo (and other organic components such as isatin or indirubin) accompanying palygorskite-associated indigo as a chromophor.[30-36]

A factor supporting the ‘dehydroindigo model’ is the similarity between the UV-Vis spectra of the specimens prepared by heating indigo with palygorskite, sepiolite, montmorillonite, etc. In

spite of several subtle, but significant differences (*vide infra*), there is a similar overall spectral profile between the different replicants, as can be seen in Figure 7, where the UV-Vis spectra of IND@PAL$_{130}$, IND@SEP$_{130}$, IND@MON$_{130}$, IND@KAO$_{130}$ are depicted. These spectra, which are comparable to those reported in literature,[20-26,33,44,49,54] include a main absorption band with maximum between 640 and 670 nm and a minor band with a more or less defined maximum between 450 and 550 nm. In the interpretation of De Faria et al.,[44] the band at ca.500 nm appears exclusively as a consequence of specific indigo-clay interactions that are responsible for a decrease in the indigo molecular symmetry and there is null dehydroindigo presence in IND@PAL$_t$ specimens.

In contrary to this interpretation, one can adduce that this specific interaction should be produced only in the channeled clays (palygorskite sepiolite) and then this band should be absent in the replicants prepared with non-channeled clays. One can see that the matching between the spectra of MB-type specimens prepared with non-channeled clays is clearly superior to that between specimens prepared with channeled clays and those prepared with non-channeled clays (See Figure S.5 in Supplementary Information). Of course, it is conceivable that in these non-channeled clays indigo may form surface complexes yielding an absorption band in the 500 nm region of wavelengths but this argument in favor of the 'all-indigo' model appears to be in contradiction with Raman data. As can be seen in Figure 2, the Raman spectra of IND@SEP$_t$, IND@MON$_t$ and IND@LAP$_t$ replicants are essentially identical to that of DHI@PAL$_t$, thus suggesting that dehydroindigo, whose spectrum displays a main absorption band just centered in the 500 nm region,[33,44] is present in a significant proportion in these specimens and participates significantly in the determination of their color. In short, if the Raman spectra of IND@PAL$_t$ specimens contain several bands coincident with those of DHI@PAL$_t$ and the UV-Vis spectrum of such specimens shows an, in principle, similar band at 500 nm, it seems more logical to admit that dehydroindigo participates in MB-type materials than attribute all these spectral signals to a peculiar, specific indigo-palygorskite complex. To treat this matter, however, there is need of considering the nature of the dye-clay association in more detail.

The dye-clay association/The binding problem

In order to analyze the UV-Vis spectra of the different DYE@CLAY hybrids, it is pertinent to

consider the problem of the association of the dyes to the clay supports. Apart from the type of binding (formation of hydrogen bonds between indigo C=O and N-H units with edge silanol units of the clay,[14] hydrogen bonding of such units (mainly C=O) with structural water,[10-12] direct bonding to Al^{3+} substituted Si^{4+} sites in tetrahedral centers[17-19] and to clay octahedral (Mg^{2+} and Al^{3+}) cations[13,16], there is common agreement in which the association of indigo to palygorskite (or sepiolite) involves the loss of zeolitic water.[10-19] The overall attachment process can be represented as:[10]

$$\{IND\} + \{pal\cdot xH_2O\} \rightarrow \{IND\cdot pal\} + xH_2O\ (l) \quad (1)$$

where {} denote solid species.

Accordingly, the usual preparation of MB simulants based on 'dry' crushing of indigo and palygorskite departs from a set of indigo microcrystals where indigo molecules form important intermolecular hydrogen bonds. Then, the formation of the hybrid material involves, in principle, the separation of individual indigo molecules from indigo crystals (in the following, 'molecularization') and their attachment to the clay. To simplify, in non-channeled clays (kaolinite, laponite, etc.) we can formally consider that an 'external' dye-clay complex is formed, consisting of molecular indigo units attached to the external surface of the clay, IND{clay}. In channeled clays (palygorskite, sepiolite), apart from the above 'external' complexes, there is possibility of (at least) a second type of attachment derived from the more or less deep penetration of the organic molecules into the clay tunnels. The formation of these 'internal' species, labeled as {IND·clay} requires, as previously noted, the release of clay's zeolitic water. For our purposes, the relevant point to emphasize is that there is possibility of (at least) 'external' and 'internal' topological redox isomers whose physicochemical properties (spectral in particular) would be different.[24-26,42,43] Accordingly, the preparation of MB-type specimens can be represented, formally, by the sequence of processes:

$$\{IND\} + \{pal\cdot xH_2O\} \rightarrow IND\{pal\cdot xH_2O\} \quad (2)$$

$$IND\{pal\cdot xH_2O\} \rightarrow \{IND\cdot pal\} + xH_2O \quad (3)$$

In the dehydroindigo modeling, this dye forms similar 'external', DHI{pal·xH$_2$O}, and 'internal' {DHI·pal} species when the parent solid dye, {DHI}, is attached to palygorskite. The corresponding processes will be:

$$\{\text{DHI}\} + \{\text{pal}\cdot x\text{H}_2\text{O}\} \rightarrow \text{DHI}\{\text{pal}\cdot x\text{H}_2\text{O}\} \quad (4)$$

$$\text{DHI}\{\text{pal}\cdot x\text{H}_2\text{O}\} \rightarrow \{\text{DHI}\cdot\text{pal}\} + x\text{H}_2\text{O} \quad (5)$$

Accordingly, we can assume that there are two indigo to dehydroindigo oxidation processes occurring in at least the external surface of the clay:

$$\text{IND}\{\text{pal}\cdot x\text{H}_2\text{O}\} + (1/2)\text{O}_2\,(\text{g}) \rightarrow \text{DHI}\{\text{pal}\cdot x\text{H}_2\text{O}\} + \text{H}_2\text{O} \quad (6)$$

and possibly also in the channels:

$$\{\text{IND}\cdot\text{pal}\} + (1/2)\text{O}_2\,(\text{g}) \rightarrow \{\text{DHI}\cdot\text{pal}\} + \text{H}_2\text{O} \quad (7)$$

Three remarks should be made: i) the above scheme will be applied regardless the question of the exact location and extent of the penetration of dye molecules into the clay tunnels of palygorskite and sepiolite; ii) there is possibility of different 'external' and different 'internal' isomers having different coordination environments; i.e. bound to silanol groups, to structural water and/or to octahedral and/or tetrahedral cations;[10-19] iii) apart from indigo and dehydroindigo, other organic components such as isatin and indirubin can coexist.[42,43]

Figure 8 depicts the thermochemical cycle which can be proposed from the perspective of the dehydroindigo model for the formation of different topological redox isomers of palygorskite-associated indigo and dehydroindigo. Although the open character of the usual preparation procedure (crushing indigo and palygorskite and heating in furnace) does not permit to consider the reaction system as closed, some of the involved thermochemical quantities can be estimated.[20,22] Solid state electrochemical data permitted to estimate the variation of Gibbs energy of indigo and dehydroindigo attachment to palygorskite, respectively corresponding to the sum of ΔG^{o} for processes described by Eqs. (2) and (3), and Eqs. (4) and (5): ΔG^{o}_{mol}(IND) + ΔG^{o}_{int}(IND) = 6±9 kJ mol^{-1} and ΔG^{o}_{mol}(DHI) + ΔG^{o}_{int}(DHI) = −72±6 kJ mol^{-1}. These

values result in an apparent Gibbs energy of indigo-palygorskite to dehydroindigo-palygorskite oxidation (Eq. (7)) of $\Delta G^{o}_{oxint} = -50\pm10$ kJ mol^{-1}. The above values, whose calculation involves several simplifying assumptions,[20,22] are in principle consistent with calculations of Chiari et al.[10] using molecular modeling, for the energy of indigo attachment to non-hydrated (–37 kJ mol^{-1}) and hydrated palygorskite (150 kJ mol^{-1}) and the average binding energy of zeolitic water calculated in optimized Maya Blue molecular models (–66.5 kJ mol^{-1}).[10,11]

There are UV-Vis, ATR-FTIR and solid state electrochemical data supporting the above scheme,[24-26,42,43] in particular, modeling solid state electrochemistry of MB[55-57]on the basis of the description of zeolite electrochemistry.[58-60] In particular, a kinetic study[55] monitoring the variation of spectral and electrochemical parameters with time during the heating of indigo (1% wt) plus palygorskite specimens indicated that the process of formation of IND@PAL$_t$ involves, at least, two successive steps. This can be seen in Figure 9 where the variation of the absorbance ratio A_{525}/A_{650} vs. heating time for IND@PAL$_{130}$, IND@PAL$_{150}$ and IND@PAL$_{180}$ specimens is depicted. In this figure one can see that the A_{525}/A_{650} ratio initially decreases, as expected (see spectra in Fig. 6) for the progress of the 'molecularization' of indigo crystals (Eq. (2)); at a given time (which is shortened on increasing temperature), the absorbance ratio increases until a stationary value is obtained. This second step can be assigned to the penetration of indigo molecules into the palygorskite channels (Eq. (3)), both steps being accompanied by the oxidation of indigo to dehydroindigo (Eqs. (6) and (7)).[55] The formation of dehydroindigo was directly supported by the application of voltammetric criteria to discriminate the oxidation state of a redox probe,[56] to solid state electrochemistry techniques.[24,25,57] In fact, recent calculations based on density functional theory are consistent with the idea that different binding arrangements for indigo and dehydroindigo in the palygorksite tunnels are possible.[61] For our purposes, the relevant aspect to underline is that the foregoing set of considerations provide an interpretative scheme for the color of MB consistent with the dehydroindigo model and kinetic data.[55]

The color of MB

Reported color graphs for indigo-palygorskite replicants from De Faria et al.,[44] indigo-zeolites (Mordenite, LTA and MFI) from Martinetto et al.,[38] and indigo-palygorskite

replicants and genuine MB archaeological samples from Calakmul taken from Garcia Moreno et al.[62] (see Supplementary Information, Figure S.6) suggest that, although the frontier between the 'blue' and 'greenish blue' samples cannot be clearly established, it appears that the greenish color is associated to specimens in which the band at 500 nm is well-developed (*vide infra*). The spectral properties of MB-type DYE@CLAY specimens can be interpreted in the dehydroindigo model on the basis of:

a) Regardless the type of clay, the non-heated IND@CLAY specimens can be described as a composite of the clay and indigo microcrystals so that the replicants retain the blue tint of the dye and the spectra equals that of solid indigo.

b) There are (at least) two different scenarios for the IND@CLAY$_t$ specimens submitted to heating above 100 ºC.

b1) In the case of laminar, non-channeled clays (montmorillonite, kaolinite, silicalite, laponite), a significant fraction of indigo converts into 'individual' molecules which bind to the clay (often forming hydrogen bridges with silanol groups of the clay or other possible interactions) whereas a minor, but significant fraction, is oxidized to dehydroindigo (and isatin and/or other organic compounds) which is also attached to the 'external' clay surface. Then, the spectrum is dominated by the absorption of 'individual' indigo molecules which is, in principle, close to that of indigo in solution, with λ_{max} around 600 nm, accompanied by the corresponding absorption of dehydroindigo individual molecules whose maximum of absorbance should be similar to those measured in solution (see Table 2); i.e., between 400 and 450 nm.

b2) In the case of MB replicants prepared from channeled clays (palygorskite, sepiolite), the heating process results in the more or less deep penetration on indigo and dehydroindigo (and other organics) into the clay tunnels. After heating, the material contains some proportion of indigo crystals 'external' to the clay grains. When the remaining indigo crystals are removed by cleaning with DMSO, acetone and/or concentrated HNO_3,[38] the spectrum consists of the contributions of the absorptions of the 'external' dyes (represented in the following for palygorskite as IND{pal}, DHI{pal}, respectively) and the absorptions of the 'internal' ones

(labeled as {IND-pal} and {DHI-pal}, respectively). In the case of indigo, the maximum of absorbance shifts to ca. 650 nm while in the case of dehydroindigo λ_{max} is displaced to ca. 500 nm.

The above interpretative scheme can be reconciled with spectral data for genuine MB samples[20,21,26,27] and synthetic replicants.[24,25,38,44] In particular: i) the excellent fit of the subtracted spectra in the region between 400 and 550 nm with the spectra of dehydroindigo forms previously commented; ii) the consistency of the subtracted spectra in the region between 550 and 800 nm with the spectra of indigo forms without loss of symmetry (absorbance maxima at 600 nm, attributable to 'external' indigo and 700 nm, attributable to 'internal' indigo).

In the context of the 'all-indigo' view, it is possible to interpret the greenish-blue color of MB as resulting exclusively from the red-shift of the indigo band at 660 nm; i.e., even if dehydroindigo is present, this compound does not contribute to the color of MB. One possible simplifying assumption is to correlate the color of the specimen with the minimum in the absorbance curve, implicitly used by Reinen et al.[54] This criterion is difficult to apply to the spectra of Maya blue specimens as can be seen in Figure 10, where the spectra of indigo (0.7 %) plus palygorskite mixtures a) unheated, and b) heated and 'cleaned' upon extraction with acetone reported by Reinen et al.[54] are reproduced. Both spectra display an absorbance maximum at ca. 660 nm, and a deeper absorbance minimum at ca. 425 nm (23500 cm^{-1}, marked by black arrows in Fig. 10). Defining an apparent absorbance minimum by extrapolating the descending branches of the absorption bands represented by dotted lines in Fig. 10 yields an apparent identical absorbance minimum at ca. 450 nm for both of the above specimens. The Maya blue specimen differs by the presence of an additional absorbance minimum at ca. 19500 cm^{-1} (513 nm, grey arrow in Fig. 10b) between the absorbance bands at ca. 660 (indigo) and 500 nm (dehydroindigo). In these circumstances, there are no clear reasons for attributing the color of MB exclusively to indigo spectral features with null contribution of dehydroindigo.

Additionally, in defense of the contribution of dehydroindigo to the color of MB one can adduce that the variation of the color coordinates (see Fig. 3 in ref.[44]) on the temperature of preparation of MB replicants parallels the variation of the ratio between the absorbance

maxima of the bands at 500 (attributed to dehydroindigo) and 660 nm (see Fig. 2 in ref.[44]) as well as the ratio between the intensities of the Raman bands at 1595 (dehydroindigo) and 1250 cm^{-1} (see Fig. 7 in ref.[44]).

The above considerations can also be regarded as consistent with data reported by Martinetto et al.[38,46] for MB-type specimens prepared by crushing indigo and different zeolites, namely MFI zeolite (silicalite, $(SiO_2)_{96}$), mordenite $[Na_8(H_2O)_{24}][Si_40A_{l8}O_{96}]$, and LTA zeolite $(Na_{96}[(AlO_2)_{48}(SiO_2)_{48}]\cdot 215H_2O)$. These authors, who interpreted their data within the frame of the 'all indigo' model, indicated that the unique replicants remaining colored after applying cleaning with concentrated HNO_3 were those prepared (2 % wt indigo) with high-silica FMI-silicalite, thus denoting that this zeolite was the unique retaining 'internal' dye molecules. Remarkably, the spectra of these specimens display solely the indigo band at ca. 620 nm (see Fig. 2f in ref.[38]) with no significant absorbance band at 500 nm. Such data are again consistent with the idea that the appearance of the greenish hue of the MB is associated to the presence of a relatively intense 500 nm band. Within the explanatory scheme presented here, the absence of this band in heated indigo plus MFI zeolite specimens would denote the absence of dehydroindigo and would be determinant, to some extent, of the maintenance of the blue color.

One plausible interpretation of these features is that, since MFI has a channel section of 5.3 × 5.6 Å, ideally sufficient to accommodate indigo molecules (of width 4.8 Å), there is entrapment of indigo molecules but no significant generation of dehydroindigo with the concomitant weakness of the 500 nm band and the absence of greenish tint. This is consistent with the position of the indigo plus zeolite specimens[38,46] in the color diagram in Figure S.6 (Supplementary Information).

Finally, it is interesting to mention that one of the arguments used by De Faria et al.[44] in support of the 'all-indigo model' is that, on comparing Raman data at different excitation wavelengths, the maximum enhancement of the band at 1595 cm^{-1} is obtained when the excitation is in resonance with the 500 nm band and that the same feature occurs with the bands at 1680, 1490 and 1461 cm^{-1} (see Fig. 6 in ref.[44]). Since the Raman bands at 1680, 1595, 1490 and 1461 cm^{-1}, as discussed in the precedent section (see in particular the spectrum of the

DHI@PAL_{130} specimen in Figure 1), can be ascribed to dehydroindigo associated to clays (palygorskite and sepiolite in particular), the more logical conclusion is that, although a contribution of the indigo-clay complex cannot be excluded, the 500 nm band can be mainly due to the absorption of clay-associated dehydroindigo rather than a hypothetic forbidden transition of indigo.

Similarly, the enhancement of the A_{500}/A_{650} ratio in the UV-Vis spectra and the area ratios of the Raman bands 1595/1250 and 1420/1250 cm^{-1} with the heating temperature of the MB-type specimens presented by De Faria et al.[44] in support of the 'all-indigo' model are also consistent with the dehydroindigo model on the basis of the respective band assignment made in previous sections.

Conjointly considered, the above results draw a picture of IND@$CLAY_t$ specimens in which the size of the channels relative to the width of the indigo molecules (4.8 Å) plays a crucial role. Then, mordenite having gross channels (7.0 × 6.5 Å) cannot retain indigo molecules; while LTA zeolite (4.1 × 4.1 Å) cannot incorporate such molecules into the channels. The intermediate cases sepiolite (10.6 × 3.7 Å) palygorskite (6.4 × 3.7 Å) and silicalite (5.3 × 5.6 Å) are characterized by the increase in the ability to trap indigo and the parallel apparent increase in the greenish tint. This can be interpreted in terms of the increase of the dehydroindigo/indigo ratio from silicalite (blue replicants, essentially null dehydroindigo) to palygorskite and sepiolite (greenish-blue replicants) because the oxidation of indigo to dehydroindigo (as indicated by Martinetto et al.[38] in their interpretation of experiments of exhaustive oxidation to isatin with concentrated HNO_3) would require a certain space (major than that provided by the silicalite channels), consistently with the relatively high activation energy derived from kinetic data.[54] This means that the oxidation of indigo to dehydroindigo would occur easily for the external isomers (Eq. (6)) but to more less (or null) extent for internal isomers (Eq. (7)), a matter needing further research.

Accordingly, the size and shape of the silicate channels appear as crucial factors for determine the color properties of MB simulants. Considering data summarized in Table 3, the indigo trapping ability increases in the SEP < PAL < SIL order while the facility for oxidizing indigo to dehydroindigo increases in the SIL < PAL < SEP order. This also explains the previously

underlined close similarity between the Raman spectra of DHI@PAL_t and IND@SEP_t replicants, clearly major than the similarity between DHI@PAL_t and IND@PAL_t ones: simply, the DHI/IND ratio would be larger in IND@SEP_t than in IND@PAL_t simulants.

Accordingly, as summarized in Figure 12, the peculiarity of palygorskite-based MB specimens derives from the compromise between the trapping ability of indigo molecules in channeled silicates and aluminosilicates (increasing on decreasing the channel effective size to approximate to the indigo molecule size) and the ability for facilitating the oxidation of indigo to dehydroindigo (increasing on increasing the channel size). Then, LTA zeolite cannot accommodate indigo molecules in its channels, being under the indigo trapping threshold. The silicalite (FMI zeolite) replicant, although just accommodating indigo molecules, does not allow a significant oxidation to 'internal' dehydroindigo (i.e., being under the indigo to dehydroindigo oxidation threshold) and, consequently, 'clean' IND@SIL_t specimens remain blue and do not provide the characteristic greenish color of the archaeological MB.

In summary, although the exact composition can vary depending the source of the materials and the preparation recipe,[23,27,28,63] the foregoing analysis of spectral data supports the view of the genuine MB as a polyfunctional organic-inorganic hybrid material in which the common presence of indigo and dehydroindigo (and other minor organic components), forming distinct topological redox isomers distributed in different locations and coordination environments in the clay support, determines the color variability, the color being mainly modulated by the dehydroindigo/indigo ratio which in turn can be controlled by the temperature of the thermal treatment.[20-26,42,43] In our view, is just this compositional and chromatic variability that defining 'genuine' MB and defines a 'MB chemistry'.[42,43,64]

Conclusions

Analysis of Raman and UV-Vis spectroscopy data in MB literature is consistent with the so-called dehydroindigo model. In particular, Raman features for all reported IND@$CLAY_t$ specimens present more or less intensively peaks common to those of the corresponding DHI@$CLAY_t$ replicants. In this view, the color of MB is determined by the common

presence of indigo and dehydroindigo. Although the contribution of other organic components and the contribution of the indigo-clay complexes cannot be excluded, the dehydroindigo/indigo ratio, which in principle increases with the temperature of the thermal treatment, appears as the main factor determining the color of the materials and its variability.

The comparative analysis of spectral data for simulants prepared from different channeled silicates: palygorskite, sepiolite, LTA, mordenite and FMI zeolites, suggests that the palygorskite channel shape and size provide the better compromise between trapping ability for indigo molecules and facility to promote the oxidation of indigo to dehydroindigo.

The current study advocates the view of MB as a polyfunctional hybrid material whose properties are determined by the presence of different organic components forming different topological redox isomers in their attachment to the silicate framework.

Acknowledgements: Project CTQ2017-85317-C2-1-P, supported with *Ministerio de Economía, Industria y Competitividad* (MINECO), *Fondo Europeo de Desarrollo Regional* (ERDF) and *Agencia Estatal de Investigación* (AEI), is gratefully acknowledged.

Supplementary Information: Figures showing the variation with temperature in Raman spectra from ref. 44, mass spectra obtained in UPLC-MS experiments and the temperature variation of the ratio between chromatographic peaks for dehydroindigo and indigo in the same from refs. 42,43 voltmmograms for different Maya blue specimens, two absorbance plots and color graphs from refs. 44,62 and a table of ^{13}C NMR data are provided.

References

(1) Merwin, H. E. in *Yucatan, Temple Warriors at Chitchen Itza*. Morris H. E.; Charlot, J.; Morris, A. A. Eds. Carnegie Institution, Washington, p. 356, 1931.

(2) Reyes-Valerio, C. *De Bonampak al Templo Mayor: el azul Maya en Mesoamérica*. Siglo XXI, México, 1993.

(3) Gómez-Romero, P.; Sánchez, C. Hybrid materials. Functional properties. From Maya Blue to 21st century materials. *New J. Chem*. **2005**, *29*, 57-58.

(4) Shepard, A. O. Maya Blue: alternative hypotheses. *Amer. Antiq*.**1962**, *27*, 565-566.

(5) Cabrera-Garrido, J. M. El 'Azul Maya', in *Informes y Trabajos del Instituto de Conservación y Restauración de Obras de Arte, Arqueología y Etnología 8*. Madrid, 1969.

(6) Magaloni, D. Materiales y técnicas de la pintura mural maya, in *Pintura mural Prehispánica en México: área maya*, De la Fuente, B.; Satines-Cicero, L. Eds. Universidad Nacional Autónoma de México, México, 2001, pp. 85-104.

(7) Arnold, D. E., Branden, J. R.; Williams, P. R.; Feinman, G. M.; Brown, J. P. The first direct evidence for the production of Maya Blue: rediscovery of a technology. *Antiquity*, **2008**, *82*,151-164.

(8) Van Olphen, H. Maya blue: a clay-organic pigment? *Science* **1967**, *154*, 645–646.

(9) Kleber, R.; Masschelein-Kleiner, R.; Thissen, J. Etude et identification du "Bleu Maya". *Stud. Conservat*. **1967**, *12*, 41-56.

(10) Chiari, G.; Giustetto R.; Ricchiardi, G. Crystal structure refinement of palygorskite and Maya Blue from molecular modelling and powder synchrotron diffraction. *Eur. J. Mineral.* **2003**, *15*, 21-33.

(11) Fois, E.; Gamba, A.; Tilocca, A. On the unusual stability of Maya blue paint: molecular dynamics simulations, *Micropor. and Mesopor. Mat.* **2003**, *57*, 263-272.

(12) Giustetto, R.; Llabres i Xamena, F. X.; Ricchiardi, G.; Bordiga, S.; Damin, A.; Gobetto R.; Chierotti, M. R. Maya Blue: A Computational and Spectroscopic Study. *J. Phys. Chem. B* **2005**, *109*, 19360-19368.

(13) Tilocca, A.; Fois, E. The Color and Stability of Maya Blue: TDDFT Calculations,*J. Phys.Chem. C* **2009**, *113*, 8683–8687.

(14) Hubbard, B.; Kuang, W.; Moser, A.; Facey, G. A.; Detellier, C. Structural study of Maya Blue: textural, thermal and solidstate multinuclear magnetic resonance characterization of the palygorskite-indigo and sepiolite-indigo adducts. *Clays Clay Miner.* **2003**, *51*, 318–326.

(15) Sánchez del Río, M.; Boccaleri, E.; Milanesio, M.; Croce, G.; van Beek, W.; Tsiantos, C.; Chyssikos, G.; Gionis, V.; Kacandes, G.; Suárez, M.; García-Romero, E. A combined synchrotron powder diffraction and vibrational study of the thermal treatment of palygorskite–indigo to produce Maya blue, *J. Mater. Sci.* **2009**, *44*, 5524-5536.

(16) Chiari, G.; Giustetto, R.; Druzik, J.; Doehne, E.; Ricchiardi, G. Pre-columbian nanotechnology: reconciling the mysteries of the maya blue pigment. *Appl. Phys. A: Mater Sci. Process.* **2008**, *90*, 3-7.

(17) Chianelli, R. R.; Perez De la Rosa, M.; Meitzner, G.; Siadati, M.; Berhault, G.; Mehta, A.; Pople, J.; Fuentes, S.; Alonzo-Nunez, G.; Polette, L. A. Synchrotron and simulations techniques applied to problems in materials science: catalysts and Azul Maya pigments,.*J. Synchr. Rad.* **2005**, *12*, 129-134.

(18) Polette-Niewold, L. A.; Manciu, F. S.; Torres, B.; Alvarado Jr, M.; Chianelli, R. R. Organic/inorganic complex pigments: Ancient colors Maya Blue. *J. Inorg. Biochem.* **2007**, *101*, 1958-1973.

(19) Fuentes, M. E.; Peña, B.; Contreras, C.; Montero, A. L.; Chianelli, R.; Alvarado, M.; Olivas, R.; Rodríguez, L. M.; Camacho, H.; Montero-Cabrera, L. A. Quantum mechanical model for Maya Blue. *Int. J. Quantum Chem.* **2008**, *108*, 1664-1673.

(20) Doménech-Carbó, A.; Doménech-Carbó, M. T.; Vázquez De Agredos-Pascual, M. L. Dehydroindigo: a New Piece into the Maya Blue Puzzle from the Voltammetry of Microparticles Approach. *J. Phys. Chem. B* **2006**, *110*, 6027-6039.

(21) Doménech-Carbó, A.; Doménech-Carbó, M. T.; Vázquez De Agredos-Pascual, M. L. Chemometric Study of Maya Blue from the Voltammetry of Microparticles Approach. *Anal. Chem.* **2007**, *79*, 2812-2821.

(22) Doménech-Carbó, A.; Doménech-Carbó, M. T.; Vázquez De Agredos-Pascual, M. L. Indigo/Dehydroindigo/Palygorskite Complex in Maya Blue: An Electrochemical Approach. *J. Phys. Chem. C* **2007**, *111*, 4585-4595.

(23) Doménech-Carbó, A.; Doménech-Carbó, M. T.; Vázquez De Agredos-Pascual, M. L. Electrochemical monitoring Maya Blue preparation from Maya's ancient procedures. *J. Solid State Electrochem.* **2007**, *11*, 1335-1346.

(24) Doménech-Carbó, A.; Doménech-Carbó, M. T.; Sanchez del Rio, M.; Goberna S.; Lima, E. Evidence of Topological Indigo/Dehydroindigo Isomers in Maya Blue-Like Complexes Prepared from Palygorskite and Sepiolite. *J. Phys. Chem. C* **2009**, *113*, 12118-12131.

(25) Doménech-Carbó, A.; Doménech-Carbó, M. T.; Sanchez del Rio, M.; Vázquez De Agredos-Pascual, M. L. Comparative study of different indigo-clay Maya Blue-like systems using the voltammetry of microparticles approach. *J. Solid State Electrochem.* **2009**, *13*, 869-878.

(26) Doménech-Carbó, A.; Doménech-Carbó, M. T.; Sanchez del Rio, M.; Vázquez De Agredos-Pascual, M. L.; Lima, E. Maya Blue as a nanostructured polyfunctional hybrid organic-inorganic material: the need to change paradigms. *New J. Chem.* **2009**, *33*, 2371-2379.

(27) Doménech-Carbó, A.; Doménech-Carbó, M. T.; Vázquez De Agredos-Pascual, M. L. Correlation between spectral, SEM/EDX and electrochemical properties of Maya Blue. A chemometric study. *Archaeometry* **2009**, *51*, 1015-1034.

(28) Doménech-Carbó, M. T.; Osete-Cortina, L.; Doménech-Carbó, A.; Vázquez de Agredos-Pascual, M. L.; Vidal-Lorenzo, C. Identification of indigoid compounds present in archaeological Maya blue by pyrolysis-silylation-gas chromatography-mass spectrometry. *J. Anal. Appl. Pyrol*. **2014**, *105*, 355-362.

(29) Doménech-Carbó, A.; Doménech-Carbó, M. T.; Vidal-Lorenzo, C.; Vázquez De Agredos-Pascual, M. L. From Maya Blue to 'Maya Yellow': A Connection between Ancient Nanostructured Materials from the Voltammetry of Microparticles. *Angew. Chem. Int. Ed.* **2011**, *50*, 5741-5744.

(30) Doménech-Carbó, A.; Doménech-Carbó, M. T.; Vidal-Lorenzo, C.; Vázquez De Agredos-Pascual, M. L. Insights into the Maya Blue Technology: Greenish Pellets from the Ancient City of *La Blanca. Angew. Chem. Int. Ed.* **2012**, *51*, 700-703.

(31) Doménech-Carbó, A.; Doménech-Carbó, M. T.; Vidal-Lorenzo, C.; Vázquez De Agredos-Pascual, M. L.; Osete-Cortina, L.; Valle-Algarra, F. M. Discovery of indigoid-containing clay pellets from La Blanca: significance with regard to the preparation and use of Maya Blue. *J. Archaeol. Sci.* **2014**, *41*, 147-155.

(32) Manciu, F. S.; Reza, L.; Polette, L. A.; Torres, B.; Chianelli, R. R. Raman and infrared studies of synthetic Maya pigments as a function of heating time and dye concentration. *J. Raman Spectrosc*. **2007**, *38*, 1193−1198.

(33) Rondão, R.; de Melo, J. S. S.; Bonifacio, V. D. B.; Melo, M. J. Dehydroindigo, the Forgotten Indigo and Its Contribution to the Color of Maya Blue. *J. Phys. Chem. A* **2010**, *114*, 1699−1708.

(34) Giustetto, R.; Wahyudi, O. Sorption of red dyes on palygorskite: Synthesis and stability of red/purple Mayan nanocomposites. *Micropor. Mesopor. Mater*. **2011**, *142*, 221-235.

(35) Giustetto, R.; Wahyudi, O.; Corazzari, I.; Turci, F. Chemical stability and dehydration behavior of a sepiolite/indigo Maya Blue pigment. *Appl. Clay Sci*. **2011**, *52*, 41-50.

(36) Ovarlez, S.; Giulieri, F.; Chaze, A.–M.; Delamare, F.; Raya, J.; Hirschinger, J. The Incorporation of Indigo Molecules in Sepiolite Tunnels. *Chem. Eur. J.* **2009**, *15*, 11326–11332.

(37) Dejoie, C.; Martinetto, P.; Dooryhée, E.; Strobel, P.; Blanca, S.; Bordat, P.; Brown, R; Porcher, F.; Sanchez del Rio, M.; Anne, M. Indigo@Silicalite: a New Organic-Inorganic Hybrid Pigment. *Appl. Mater. Interf.* **2010**, *2*, 2308–2316.

(38) Dejoie, C.; Dooryhée, E.; Martinetto, P.; Blanc, S.; Bordat, P.; Brown, R.; Porcher, F.; Sanchez del Rio, M.; Strobel, P.; Anne, M.; Van Eslande, E.; Walter, P. Revisiting Maya Blue and Designing Hybrid Pigments by Archaeomimetism. hal-00495128.v1,http://hal.archives-ouvertes.fr/.

(39) Ovarlez, S.; Giulieri, F., Delamare, F.; Sbirrazzuoli, N.; Chaze, A. –M. Indigo–sepiolite nanohybrids: Temperature-dependent synthesis of two complexes and comparison with indigo–palygorskite systems. *Micropor. Mesopor. Mater*. **2011**, *142*, 371-380.

(40) Tsiantos, C.; Tsampodimou, M.; Kacandes, G. H.; Sánchez del Río, M.; Gionis, V.; Chryssikos, G. D. Vibrational investigation of indigo−palygorskite association(s) in synthetic Maya blue. *J. Mater. Sci*. **2012**, *47*, 3415-3428.

(41) Wiedemann, H. G.; Brzezinka,, K. –W.; Witke, K.; Lamprecht, I. Thermal and Raman-spectroscopic analysis of Maya Blue carrying artefacts, especially fragment IV of the Codex Huamantla. *Thermochim. Acta* **2007**, *456*, 56-63.

(42) Doménech-Carbó, A.; Doménech-Carbó, M. T.; Valle-Algarra, F. M.; Domine, M. E.; Osete-Cortina. L. On the dehydroindigo contribution to Maya Blue. *J. Mater. Sci.* **2013**, *48*, 7171-7183.

(43) Doménech-Carbó, A.; Valle-Algarra, F. M.; Doménech-Carbó, M. T.; Domine, M. E.; Osete-Cortina. L.; Gimeno-Adelantado, J. V. Redox tuning and species distribution in Maya Blue-type materials: a reassessment. *Appl. Mater. Sci. Interf.* **2013**, *5*, 8134-8145.

(44) Bernardino, N. D.; Constantino, V. R. L.; De Faria, D. L. A. Probing the Indigo Molecule in Maya Blue Simulants with Resonance Raman Spectroscopy. *J. Phys. Chem. C* **2018**, *122*, 11505-11515.

(45) Sánchez del Río, M.; Picquart, M.; Haro-Poniatowski, E.; van Eslande, E.; Uc, V.H. On the Raman spectrum of Maya blue. *J. Raman Spectrosc.* **2006**, *37*, 1046-1053.

(46) Dejoie, C.; Martinetto, P.; Doryhée, E.; Van eslande, E.; Blanc, S.; Bordat, P.; Brown, R.; Porcher, F.; Anne, M. Association of Indigo with Zeolites for Improved Color Stabilization. *Appl. Spectr*. **2010**, *64*, 1131-1138.

(47) Leona, M.; Casadio, F.; Bacci, M.; Picollo, M. Identification of the Pre-Columbian Pigment Maya Blue on Works of Art by Noninvasive UV-Vis and Raman Spectroscopic Techniques. *J. Am. Inst. Conserv*. **2004**, *43*, 39−54.

(48) Vandenabeele, P.; Bodé, S.; Alonso, A.; Moens, L. Raman spectroscopic analysis of the Maya wall paintings in Ek'Balam, Mexico. *Spectrochim. Acta, Part A* **2005**, *61*, 2349−2356.

(49) Garcia Moreno, R.; Strivay, D.; Gilbert, B. Maya blue−green pigments found in Calakmul, Mexico: a study by Raman and UV−visible spectroscopy. *J. Raman Spectrosc.* **2008**, *39*, 1050−1056.

(50) Doménech-Carbó, A.; Doménech-Carbó, M. T.; Edwards, H. G. M. On the interpretation of the Raman spectra of Maya Blue: a review on the literature data. *J. Raman Spectrosc.* **2011**, *42*, 86−96.

(51) Tomkinson, J.; Bacci, M.; Picollo, M.; Colognesi, D. The vibrational spectroscopy of indigo: A reassessment. *Vibrat .Spectrosc.* **2009**; *50*, 268-276.

(52) Witke, K.; Brzezinka, K.-W.; Lamprecht, I. Is the indigo molecule perturbed in planarity by matrices? *J. Mol. Struct.* **2003**, *661−662*, 235−238.

(53) Bernardino, N. D.; Brown-Xu, S.; Gustafson, T. L.; , D. L. A. Time-Resolved Spectroscopy of Indigo and of a Maya Blue Simulant. *J. Phys. Chem. C* **2016**, *120*, 21905-21914.

(54) Reinen, D.; Köhl, P.; Müller, C. The Nature of the Colour Centres in 'Maya Blue' the Incorporation of Organic Pigment Molecules into the Palygorskite Lattice. Z. Anorg. Allg. Chem. 2004, 630, 97−103.

(55) Doménech-Carbó, A.; Doménech-Carbó, M.T.; Osete-Cortina, L.; Montoya, N. Application of solid-state electrochemistry techniques to polyfunctional organic-inorganic hybrid materials: the Maya Blue problem. *Micropor. Mesopor. Mater.* **2013**, *166*, 123-130.

(56) Scholz, F.; Hermes, M. The determination of the redox state of a dissolved depolariser by cyclic voltammetry in the case of electrochemically reversible systems. *Electrochem. Commun.* **1999**, *1*, 345-348.

(57) Doménech-Carbó, A.; Martini, M.; De Carvalho, L. M.; Doménech-Carbó, M. T. Square wave voltammetric determination of the redox state of a reversibly oxidized/reduced depolarizer in solution and in solid state. *J. Electroanal. Chem.* **2012**, *684*, 13-19.

(58) Doménech-Carbó, A.; Foermentín, P.; García, H.; Sabater, M. J. On the existence of different zeolite-associated topological redox isomers. Electrochemistry of Y zeolite.associated Mn(salen)N_3 complex. *J. Phys. Chem. B* **2002**, *106*, 574-582.

(59) Doménech-Carbó, A. A model for solid-state voltammetry of zeolite-associated species. *J. Phys. Chem. B* **2004**, *108*, 20471-20478.

(60) Doménech-Carbó, A.Theoretical scenarios for the electrochemistry of porous silicate-based materials: an overview. *J. Solid State Electrochem.* **2015**, *19*, 1887-1903.

(61) Sánchez-Ochoa, F.; Cocoletzi, G.H.; Canto, G. Trapping and diffusion of organic dyes inside of palygorskite clay: The ancient Maya Blue pigment. *Micropor. Mesopor. Mater.* **2017**, *249*, 111-117.

(62) Garcia Moreno, R.; Strivay, D.; Gilbert, B. Maya blue-green pigments found in Calakmul, Mexico: a study by Raman and UV-visible spectroscopy. *J. Raman Spectr*. **2008**, *39*, 1050-1056.

(63) Lima, E.; Guzmán, A.; Vera, M.; Rivera, J. L.; Fraissard, J. Aged Natural and Synthetic Maya Blue-Like Pigments: What Difference Does It Make?*J. Phys. Chem. C* **2012**, *116*, 4556–4563.

(64) Doménech-Carbó, A.; Valle-Algarra, F. M.; Doménech-Carbó, M. T.; Osete-Cortina, L.; Domine, M. 'Maya Chemistry' of Organic-inorganic Hybrid Materials: Isomerization, Cyclicization and Redox Tuning of Organic Dyes Attached to Porous Silicates. *RSC Adv.* **2013**, *3*, 20099-21005.

Table 1. Raman bands for MB specimens taken from literature data.[44-46,52,53] The band at 1634 cm^{-1} can also be attributed to C=N vibration.[50]

υ (cm^{-1})	**Assign.[44,45,52,53]**	**IND Solid[45,52]**	**IND in DMSO[44]**	**IND @ PAL$_{130}$[44]**	**IND @ SEP$_{130}$[44]**	**DHI @ PAL$_{130}$[44]**	**DHI solid[44,46]**
1732	ν(C=C) ν(C=O)						■
1698	ν(C=C) ν(C=O)	■	■				
1680	ν(C=C)(ν(C=O)δ(N-H))	■		■	■	■	
1627-1634*	δ(C-C)δ(C-H)	■	■	■	■	■	
1595	δ(C-C$_{ring}$) ν(C-C) δ(N-H)			■	■	■	■
1582	ν(C=C) ν(C=O)	■	■				
1574	ν(C-C)	■	■	■	■	■	
1530	ν (N=C-C=N)	■			■		■
1490	ν(C-C) δ(C-H)			■	■	■	
1461-1448	δ(C-H) δ(C-C$_{ring}$) δ(N-H)	■	■	■	■	■	■
1420				■	■	■	
1378	δ (N=C-C=N)			■	■	■	■
1361	δ(N-H)δ(C-H)	■	■	■	■	■	
1316	δ(C-H)δ(C=C)	■	■	■			
1250	δ(C-H)δ(C=C) δ(N-H)	■	■	■	■	■	

Table 2. Literature data for the UV-Vis spectra of different studied systems. λ_{max} denotes the wavelength at which there is a maximum of absorbance in the corresponding spectrum. The hybrid materials are labeled as DYE@CLAY$_t$, where t is the temperature (ºC) at which the specimen was prepared, DYE = IND (indigo) and DHI (dehydroindigo) and CLAY = LAP (laponite), MON (montmorillonite), PAL (palygorskite), SEP (sepiolite).

System	**λ_{max} (nm)**	**λ_{max} (nm)**	**Source**
Indigo in solution	600 (toluene),[33] 607 (methanol),[33] 620 (DMSO)[60]		Seixas de Melo et al.[33] and De Faria et al.[60]
IND@PAL$_{130}$	667 667	435 500	Reinen et al.[54] De Faria et al.[44]
IND@SEP$_{130}$	642	500	De Faria et al.[44]
IND@MON$_{130}$	646	456	De Faria et al.[44]
IND@LAP$_{130}$	642	ca. 460	De Faria et al.[44]
Dehydroindigo in solution		455 (toluene),[33] 400 (methanol),[33] 450 ($CHCl_3$)[53]	Seixas de Melo et al.[33]; De Faria et al.[53]
DHI@LAP$_{130}$		515	De Faria et al.[53]
DHI@PAL		528	Seixas de Melo et al.33

Table 3. Summary of the variation of the color properties of IND@CLAY$_t$ specimens in the dehydroindigo model combining data from different sources.[38,43] [a] color of the heated specimens (*t* between 130 and 180 ºC) prepared by crushing indigo (1-2 % wt) plus clay mixtures; [b] color of the heated specimens after cleaning with DMSO and/or acetone and/or concentrated HNO_3.

Clay	Tunnel dimensions (Å)	Tunnel section area (Å^2)	color[a]	color[b]
LTA zeolite	4.1 × 4.1	16.81	blue	yellow[38]
silicalite	5.3 × 5.6	29.68	blue	blue/violet[38]
palygorskite	6.4 × 3.7	23.68	greenish-blue	greenish-blue[35,43]
sepiolite	10.6 × 3.7	39.22	greenish-blue	greenish-blue[35,43]
mordenite	7.0 × 6.5	45.5	greenish-blue	white[38]

Figures

Figure 1. Raman spectra of: a) indigo in DMSO solution (λ_o = 532 nm) after subtraction of the solvent spectrum, b) IND@PAL$_{130}$ (λ_o = 632.8 nm), c) solid dehydroindigo, d) IND@PAL$_{130}$ and e) DHI@SEP (all three using λ_o = 457.9 nm) in the 1200 to 1800 cm^{-1} region. Adapted from De Faria et al.[44]

Figure 2. a) Raman spectra recorded at λ_o = 785 nm, for i) synthetic indigo and synthetic specimens ii) IND@SEP$_{150}$ and iii) IND@PAL$_{150}$. b) Detail of the region between 500 and 1000 cm^{-1} after background subtraction.

Figure 3. Raman spectra from four blue spots of the Maya clay head fragment (Catalog No. IVCa 21166, Ethnological Museum in Berlin), excitation wavelength 514.5 nm, taken from Lamprecht et al.[41] The continuous arrows mark the Raman features coincident with those recorded for DHI@PAL$_t$ replicants and the dotted arrows mark the N-H characteristic band absent or almost entirely absent in these spectra as expected for samples containing a significant proportion of dehydroindigo.

Figure 4. LC-UV chromatograms of: a) indigo solution in DMSO and DMSO extracts of b) IND@PAL$_{140}$ and IND@PAL$_{180}$. d-f) UV-Vis spectra of the eluted aliquots of the chromatogram c) for indigo (a), isatin (b) and dehydroindigo (c). Inset: photographic images[42] of the extracts of a IND@KAO specimen using, from left to right, 90:10 (v/v) H_2O:MeOH, 50:50 (v/v) MeOH:DMSO, and DMSO.

Figure 5. UV-Vis spectra of: a) indigo in DMSO solution, b) dehydroidnigo in DMSO solution, c) solid indigo, and d) IND@PAL$_{130}$. The Gaussian components after deconvolution of the spectra are also depicted as fine continuous lines, and their sum is depicted as a dotted line. The arrows mark the possible common components of indigo (blue) and dehydroindigo (green) in different spectra.

Figure 6. ^{13}C CPMAS spectra of the sepiolite–indigo (11.5 wt% indigo) mixture. Thermal treatment: (a) unheated; heated for 10 min at (b) 180 ºC, (c) 280 ºC, (d) 350 ºC. Adapted from

Giulieri et al.[39]

Figure 7. UV-Vis spectra of a) IND@PAL$_{130}$, b) IND@SEP$_{130}$, c) IND@MON$_{130}$, and d) IND@KAO$_{130}$. The black arrow marks the absorption band at ca. 660 nm assigned to indigo species and the white arrow marks the 450-500 nm absorption band attributable to the absorption of dehydroindigo species.

Figure 8. Thermochemical cycle for the formation of different topological redox isomers of palygorskite-associated indigo and dehydroindigo.

Figure 9. Time variation of the A_{525}/A_{650} ratio in the VIS spectra of 1% (w/w) indigo + palygorskite specimens treated at 130, 150 and 180 ºC. Adapted from Doménech-Carbó et al.[55] correcting erroneous labeling in the original figure.

Figure 10. Spectra of: a) unheated, and b) heated and extracted indigo(0.7 %) plus palygorskite mixtures reported by Reinen et al.[54] The black arrow marks the maximum of absorbance at ca. 660 nm and the white arrow the absorbance band at 500 nm. The dotted black arrow marks the deeper absorbance minimum at ca. 425 nm and the grey arrow the minimum at ca. 570 nm resulting from the intersection of the 660 and 500 nm bands. The dotted lines extrapolate the absorption bands to define an apparent minimum at ca. 450 nm (see text).

Figure 11. Schematic representation of the variation of the properties of IND@CLAY replicants prepared by crushing indigo with channeled clays depending on the size of the clay channels relative to the indigo molecule. Formally, indigo experiences a two-proton, two-electron oxidation to dehydroindigo.

Figure 1.

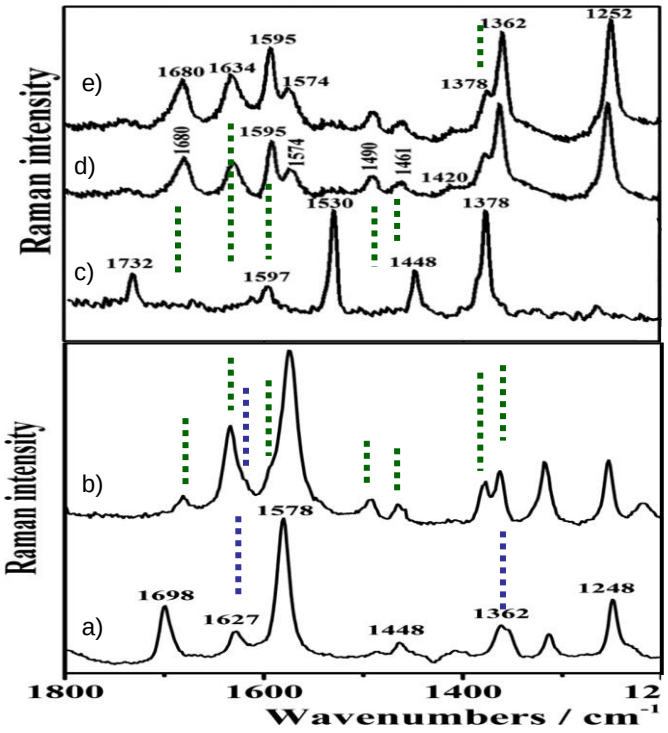
Raman intensity
e)
1680
1634
1595
1574
1378
1362
1252
d)
1680
1595
1574
1490
1461
1420
1530
1378
c)
1732
1597
1448
Raman intensity
b)
1578
a)
1698
1627
1448
1362
1248
1800
1600
1400
12
Wavenumbers / cm⁻¹

Figure 2.

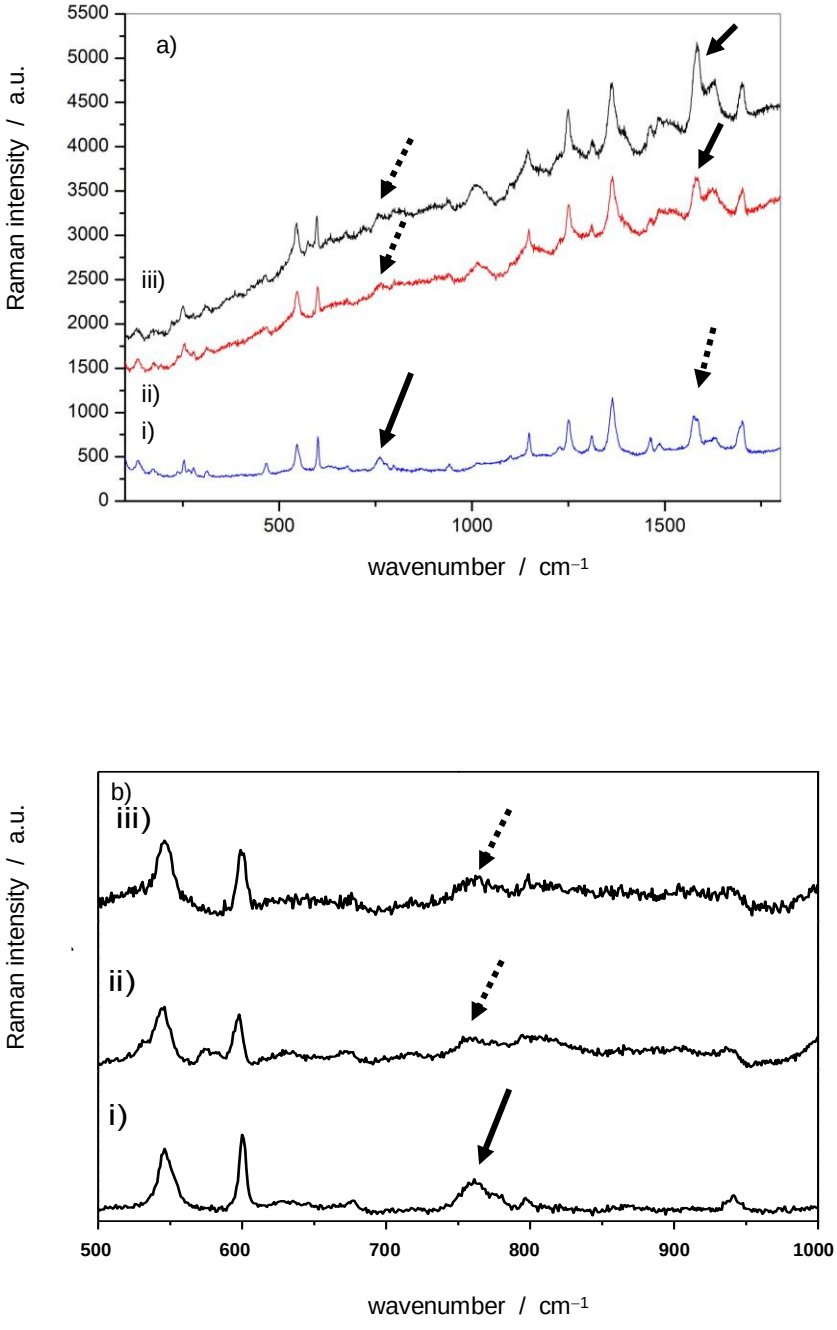
a)
iii)
ii)
i)
Raman intensity / a.u.
wavenumber / cm⁻¹
b)
iii)
ii)
i)
Raman intensity / a.u.
wavenumber / cm⁻¹

Figure 3.

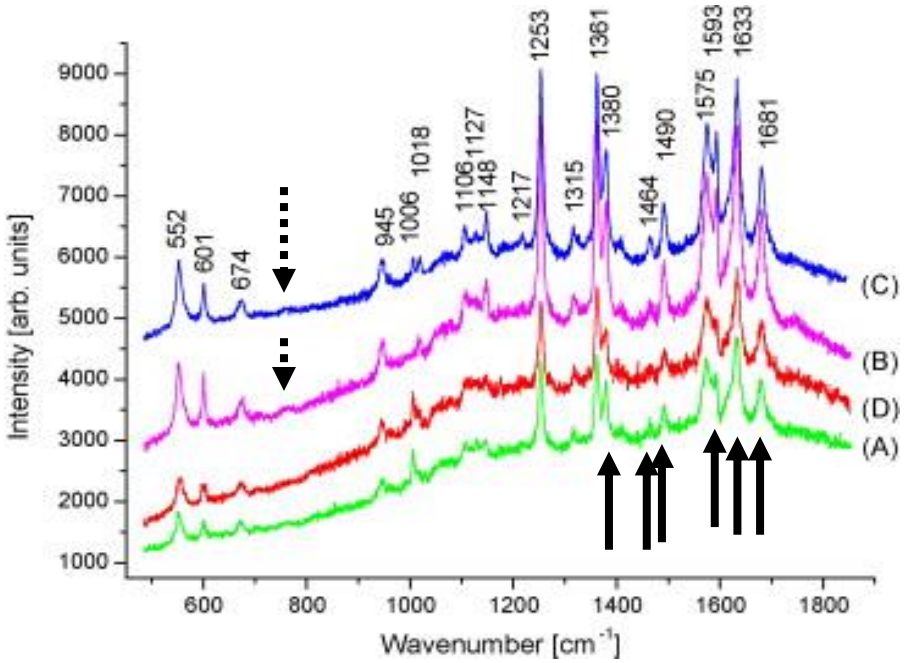
Intensity [arb. units]
Wavenumber [cm^{-1}]
552
601
674
945
1006
1018
1106
1127
1148
1217
1253
1315
1361
1380
1464
1490
1575
1593
1633
1681
(C)
(B)
(D)
(A)

Figure 4.

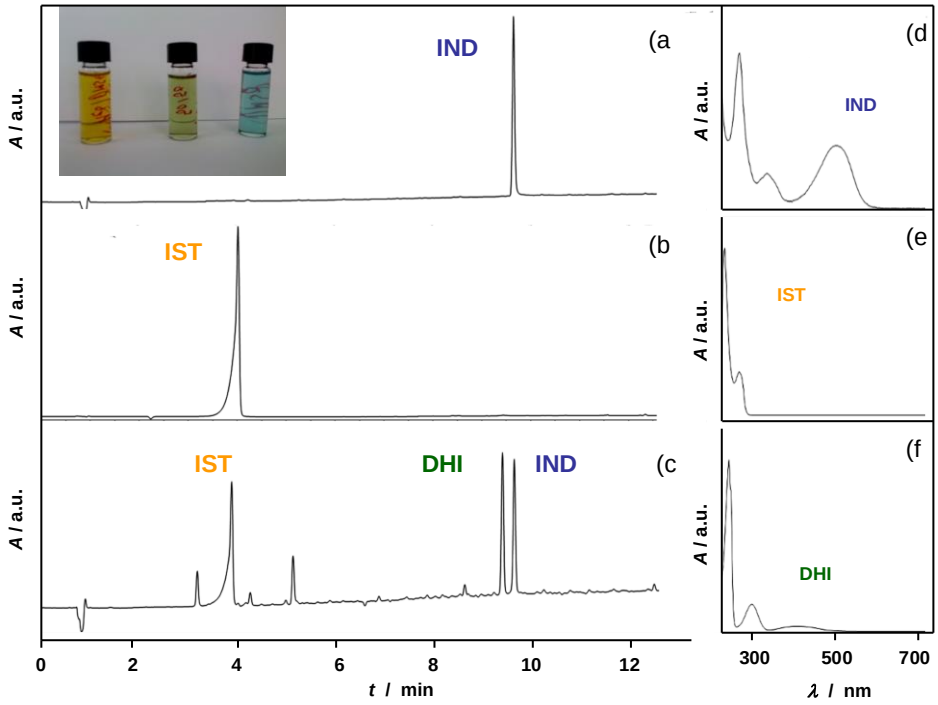
IND
(a
IST
(b
IST
DHI
IND
(c
A / a.u.
0
2
4
6
8
10
12
t / min
(d
IND
(e
IST
(f
DHI
300
500
700
λ / nm

Figure 5.

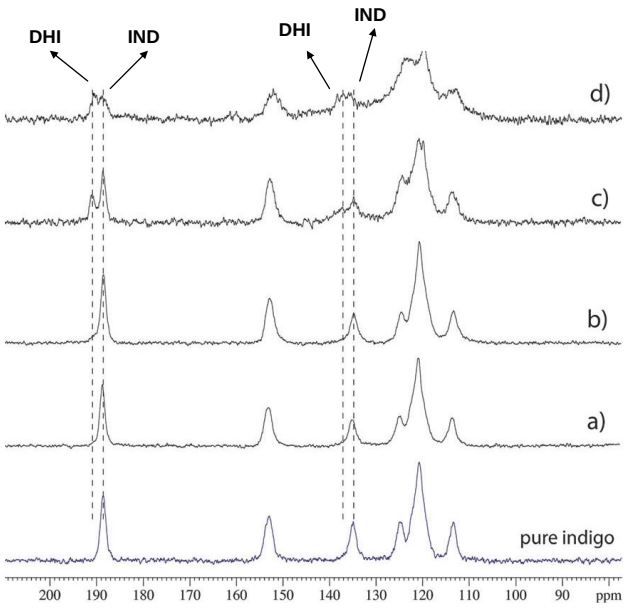
DHI
IND
DHI
IND
d)
c)
b)
a)
pure indigo
200
190
180
170
160
150
140
130
120
110
100
90
ppm

Figure 6.

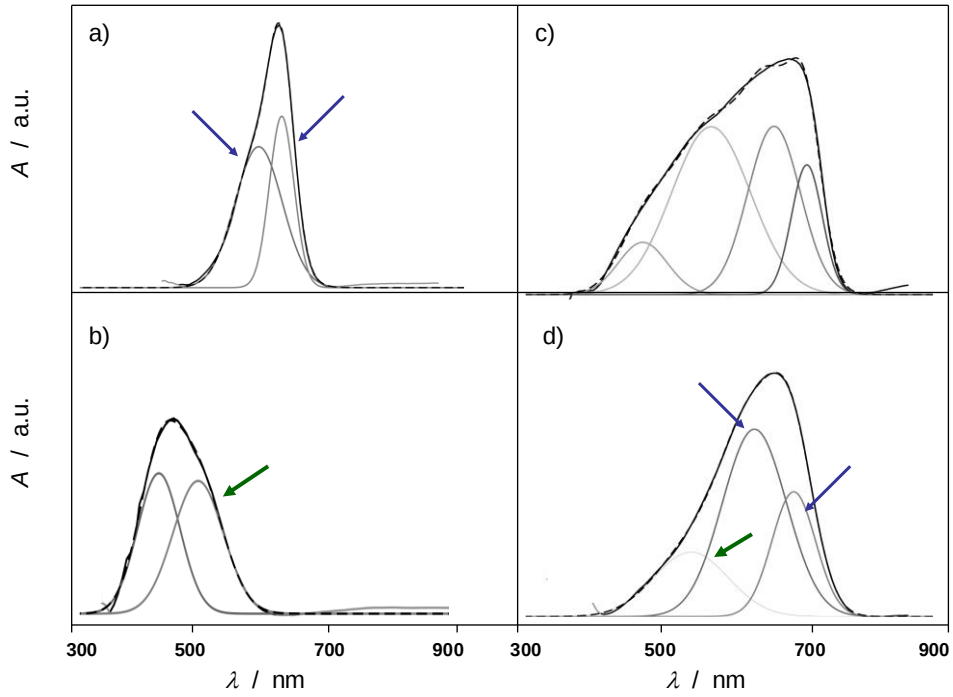

Figure 7.

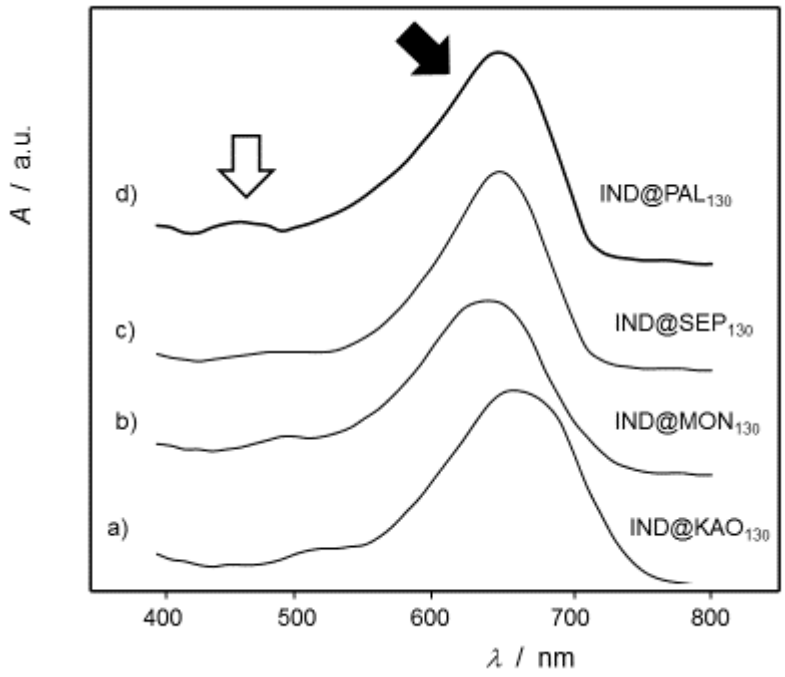
A / a.u.
d)
IND@PAL130
c)
IND@SEP130
b)
IND@MON130
a)
IND@KAO130
400
500
600
700
800
λ / nm

Figure 8.

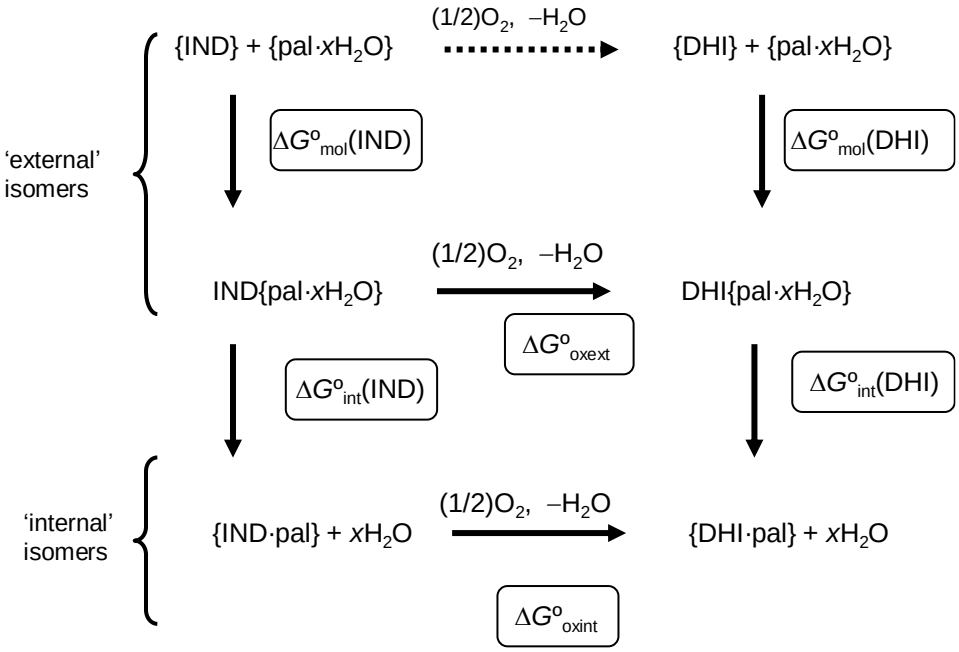
(1/2)O2, –H2O
{IND} + {pal·xH2O}
{DHI} + {pal·xH2O}
ΔGomol(IND)
ΔGomol(DHI)
'external' isomers
(1/2)O2, –H2O
IND{pal·xH2O}
DHI{pal·xH2O}
ΔGooext
ΔGoint(IND)
ΔGoint(DHI)
'internal' isomers
(1/2)O2, –H2O
{IND·pal} + xH2O
{DHI·pal} + xH2O
ΔGooint

Figure 9.

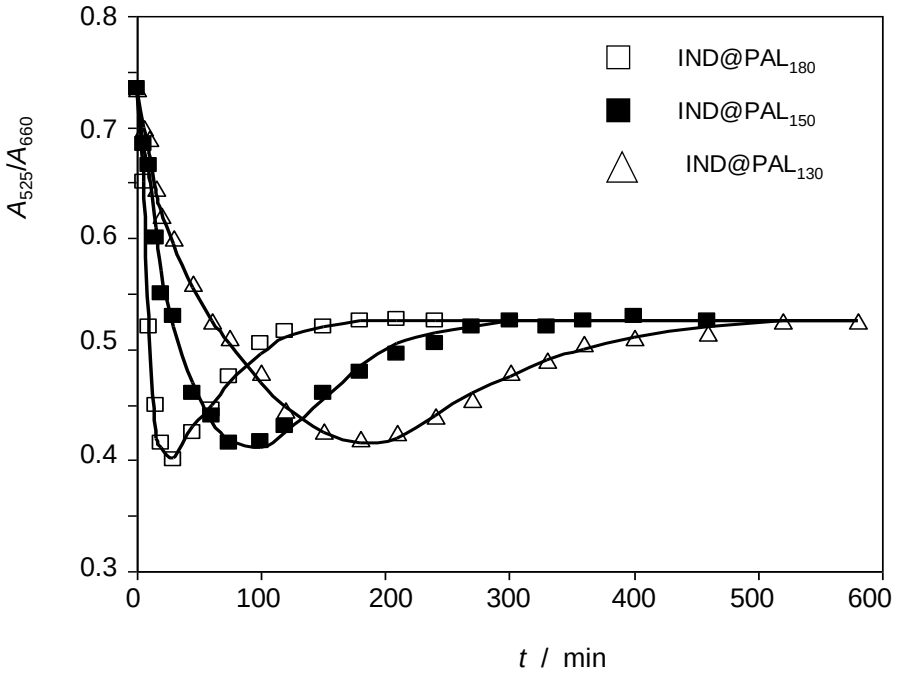
0.8
0.7
0.6
0.5
0.4
0.3
0
100
200
300
400
500
600
A_{525}/A_{660}
t / min
IND@PAL$_{180}$
IND@PAL$_{150}$
IND@PAL$_{130}$

Figure 10.

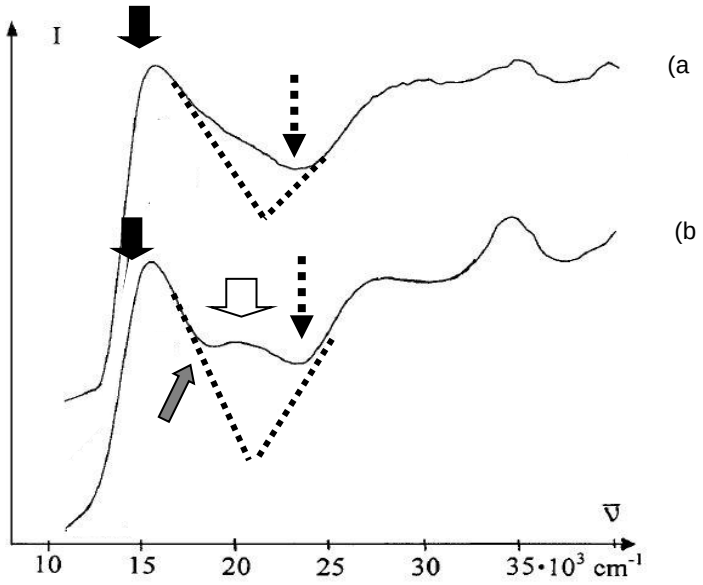

Figure 11.

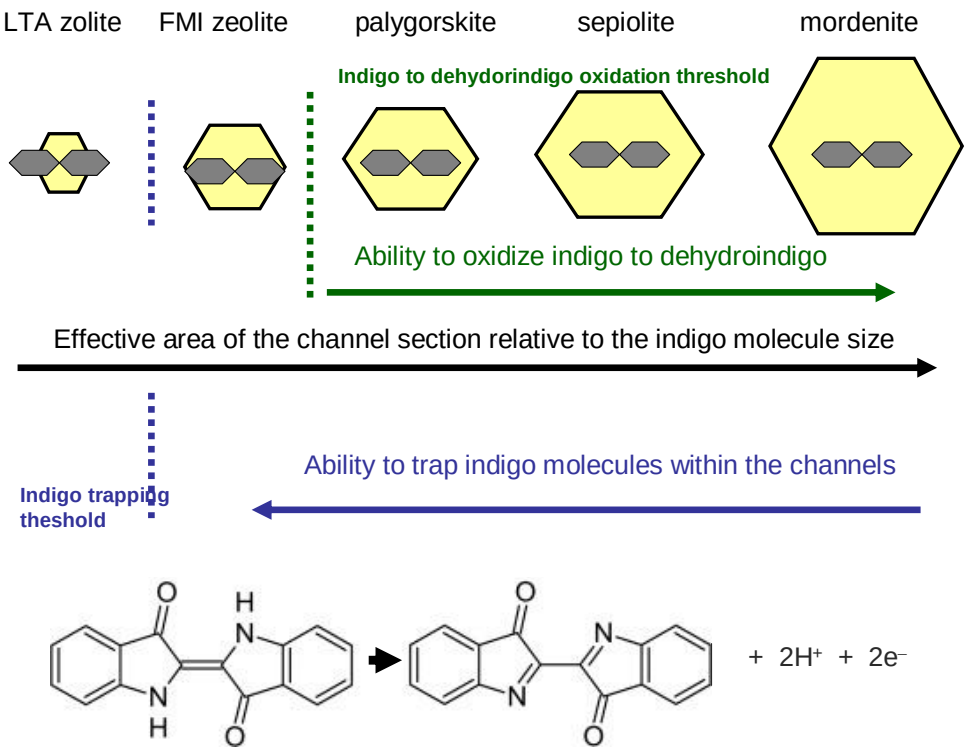
LTA zolite
FMI zeolite
palygorskite
sepiolite
mordenite
Indigo to dehydorindigo oxidation threshold
Ability to oxidize indigo to dehydroindigo
Effective area of the channel section relative to the indigo molecule size
Ability to trap indigo molecules within the channels
Indigo trapping theshold
+ 2H+ + 2e–